

# IRSp53/Eps8 Complex Is Important for Positive Regulation of Rac and Cancer Cell Motility/Invasiveness

Yosuke Funato,<sup>1,2</sup> Takeshi Terabayashi,<sup>1</sup> Naoko Suenaga,<sup>3</sup> Motoharu Seiki,<sup>3</sup> Tadaomi Takenawa,<sup>2</sup> and Hiroaki Miki<sup>1,4</sup>

<sup>1</sup>Division of Cancer Genomics, <sup>2</sup>Biochemistry, and <sup>3</sup>Cancer Cell Research, Institute of Medical Science, University of Tokyo, Tokyo, Japan, and <sup>4</sup>PRESTO, Japan Science and Technology Agency, Kawaguchi, Saitama, Japan

## ABSTRACT

IRSp53 has been characterized as an adaptor protein that links Rho-family small GTPases, such as Rac, to reorganization of the actin cytoskeleton. Here, we search for other binding partners for the IRSp53 SH3 domain and identify Eps8 as the major binding protein in fibroblasts and various cancer cell lines. Eps8 has been shown to form a Rac-specific guanine nucleotide exchange factor complex with Abi-1 and Sos-1, which seems essential for ruffling formation induced by oncogenic Ras. We confirm the IRSp53/Eps8 complex formation *in vivo* and the direct association between Eps8 NH<sub>2</sub>-terminal proline-rich sequence and IRSp53 SH3 domain. This complex synergistically activates Rac by reinforcing the formation of the Eps8/Abi-1/Sos-1 Rac-guanine nucleotide exchange factor complex, which mediates positive regulation of Rac activity. In addition, IRSp53/Eps8 complex formation as determined by fluorescent resonance energy transfer analysis, occurs at the leading edge of motile cells, and the motility and invasiveness of HT1080 fibrosarcoma cells are suppressed by inhibiting complex formation. These findings implicate the importance of the IRSp53/Eps8 complex in Rac activation and metastatic behavior of the malignant tumor cells.

## INTRODUCTION

Increased cell motility and invasiveness are key steps for metastasis of the tumor cells. Rac, a Rho-family small GTPase is known as a critical regulator of membrane ruffling caused by actin cytoskeleton rearrangement, and it has also shown to be involved in tumor metastasis (1–3). WAVE2 is a WASP family actin-polymerizing protein that is essential for Rac-dependent membrane ruffling, directed migration, and cardiovascular development (4–8). Rac does not bind directly to WAVE2, but it interacts instead in an indirect manner through IRSp53 (9–11).

IRSp53 has been best characterized as an adaptor protein between Rho-family small GTPases and actin cytoskeleton reorganizing proteins. In addition to Rac and WAVE2, Cdc42 binds to IRSp53 and stimulates filopodium formation through Mena (12, 13). Shank1 is also linked to Cdc42 through IRSp53, and mDia, a target protein for Rho, binds to IRSp53 in a Rho-GTP-dependent manner (14–16).

Eps8 was identified first as a substrate of the epidermal growth factor receptor (17). It has been reported that overexpression of Eps8 leads to increased mitogenic signaling and malignant transformation (17–19). Enhanced expression and tyrosine phosphorylation of Eps8 has been detected in tumors and transformed cell lines (18, 20, 21). At the molecular level, Eps8 has been reported to bind Abi-1 and Sos-1 and forms a trimolecular Rac-guanine nucleotide exchange factor complex (22, 23), which is important for passing the signal from Ras and phosphatidylinositol 3'-kinase (PI3k) to Rac (24, 25).

We performed a comprehensive search for IRSp53-binding proteins

by pull-down assay. Here, we report that Eps8 is the major binding protein for IRSp53 in both fibroblasts and cancer cells. We also show that the IRSp53/Eps8 complex mediates Rac activation and seems to be important for cell motility and invasion.

## MATERIALS AND METHODS

**Antibodies.** We used antibodies for IRSp53 (9), Myc-tag (Santa Cruz Biotechnology, Inc., Santa Cruz, CA), FLAG-tag (Sigma Chemical Co., St. Louis, MO), Eps8 (BD Biosciences, San Jose, CA), Sos-1 (Santa Cruz Biotechnology), actin (Molecular Probes, Inc., Eugene, OR), and Rac (a generous gift from Dr. Toshifumi Azuma, Keio University Medical School, Tokyo, Japan).

**Construction of Mutant IRSp53 and Eps8.** IRSp53-RCB, -middle, and -CT were prepared previously (9). IRSp53-SH3 and - $\Delta$ SH3 were constructed by digesting the CT fragment with PstI restriction enzyme. Eps8-Pr and Eps8-Cont were prepared by inserting chemically synthesized oligonucleotides. The other fragments of mouse Eps8 were constructed by inserting the corresponding fragments amplified by PCR.

**Cell Culture and Transfection.** The following cell lines were used: B16 melanoma cells (the Cell Resource Center for Biomedical Research, Tohoku University, Sendai, Japan); and HT1080 fibrosarcoma cells and MCF-7 breast adenocarcinoma cells (Japanese Collection of Research Bioresources, Osaka, Japan). NIH3T3 cells, COS7 cells, and A431 cells were maintained routinely in our laboratory. NIH3T3, COS7, and HT1080 cells were transfected by LipofectAmine2000, LipofectAMINE (Invitrogen Corp., Carlsbad, CA), and FuGENE 6 (Roche Applied Science, Indianapolis, IN), respectively.

**The [<sup>35</sup>S]-Labeling.** The 280  $\mu$ Ci (10 MBq) Redivue Pro-mix L-[<sup>35</sup>S] *in vitro* cell labeling mix (Amersham Biosciences, Piscataway, NJ) was used for cells in each 150-mm diameter dish. Labeled proteins were detected by autoradiography with a BAS2000 imaging analyzer (Fujifilm, Tokyo, Japan).

**Rac Activation Assay.** We used 15  $\mu$ g of plasmid for transfection of COS7 cells in a 150-mm diameter dish. As an indicator of Rac activation status, 3  $\mu$ g of pEFBOS-Myc-Rac-WT was always included. The remaining 12  $\mu$ g was divided equally for each plasmid (indicated in Fig. 3, A and B and Fig. 4, A and B). Twenty-four h after transfection, the medium was replaced and starved for 24 h. Lysates were mixed with 100  $\mu$ g of glutathione S-transferase (GST)-PAK-Cdc42- and Rac-interactive binding (CRIB) immobilized on glutathione-Sepharose beads (Amersham Biosciences). After 45 min of rotation, the beads were washed, and bound proteins were analyzed. The results for three independent experiments were quantified by measuring the band of interest with densitometer. The activity of Rac was evaluated by dividing the amount of Rac precipitated with PAK-CRIB by the amount of Rac in the lysate. The average and SE of three independent experiments were calculated. For the detection of activated endogenous Rac, confluent cells on 150-mm diameter dishes were starved for 24 h and used.

**Imaging of Fluorescent Resonance Energy Transfer (FRET) Efficiency Inside the Migrating Cells.** Twenty-four h after transfection, a wound was made by scraping the cell monolayer across the dish with a pipette tip to generate motile NIH3T3 cells. Then, cells were incubated for an additional 8 h and observed with a TCS-SP2 confocal microscope ( $\times$ 63 objective; Leica Microsystems K.K., Tokyo, Japan). FRET measurement was performed with FRET acceptor photobleaching program of the Leica confocal software, according to the manufacturer's instructions.

**Migration/Invasion Assays.** Phagokinetic motility assays, migration assays, and invasion assays were performed as described previously (8, 26). Cells were photographed with an Axiovert S10 inverted phase-contrast microscope (Carl Zeiss).

**Statistics.** All of the *P*s were determined according to Student's *t* test.

Received 2/2/04; revised 4/30/04; accepted 5/26/04.

**Grant support:** Grant-in-Aid for Cancer Research from the Ministry of Education, Science, and Culture of Japan.

The costs of publication of this article were defrayed in part by the payment of page charges. This article must therefore be hereby marked *advertisement* in accordance with 18 U.S.C. Section 1734 solely to indicate this fact.

**Requests for reprints:** Hiroaki Miki, Division of Cancer Genomics, Institute of Medical Science, University of Tokyo, 4-6-1 Shirokanedai, Minato-ku, Tokyo 108-8639, Japan. Phone: 81-3-5449-5657; Fax: 81-3-5449-5676; E-mail: miki@ims.u-tokyo.ac.jp.

**RESULTS**

**Identification of Eps8 as an IRSp53 SH3-Binding Protein.** We performed pull-down assays to identify novel binding proteins for the IRSp53 SH3 domain in various cell lines. Lysates from [<sup>35</sup>S]-labeled A431, B16, HT1080, MCF-7, and NIH3T3 cells were incubated with GST-IRSp53-CT containing a SH3 domain (schematic is shown in Fig. 1A). Bound proteins were visualized by autoradiography. We identified a major bound protein of ~95 kDa in all of the cell lines (Fig. 1B). By MALDI-TOF-MS, we identified this protein as Eps8.

**In Vivo and in Vitro Binding between IRSp53 and Eps8.** To confirm the *in vivo* interaction between IRSp53 and Eps8, coimmunoprecipitation analysis was performed. We observed a significant Eps8 signal in the anti-IRSp53 precipitates but not in the preimmune rabbit serum precipitates, confirming the *in vivo* complex formation between IRSp53 and Eps8 (Fig. 2A).

We investigated next at which regions of IRSp53 and Eps8 this interaction occurs. Various truncated fragments of IRSp53 were prepared as GST-fusion forms (Fig. 2B), and pull-down assays were performed. We observed positive Eps8 signals in GST-IRSp53-WT, -CT, and -SH3 precipitates, indicating that Eps8 binds to the SH3 domain of IRSp53 (Fig. 2C). To determine the binding site of Eps8, Eps8 was divided into four fragments (Eps8-1–Eps8-4; Fig. 2B),

which were expressed as FLAG-tagged forms in COS7 cells. In pull-down assays with GST-IRSp53-CT, there were strong positive signals for FLAG-Eps8-WT and FLAG-Eps8-1 (Fig. 2C). This result indicates that Eps8 binds to IRSp53 via the NH<sub>2</sub>-terminal region, which includes a proline-rich sequence (amino acids 207–221). Then, we divided Eps8-1 into several regions that contain or do not contain this proline-rich sequence (Eps8-1-1–Eps8-1-3, Eps8-Pr, Eps8-Cont, and Eps8-1-ΔPr; Fig. 2B) and performed pull-down assays with these GST-tagged Eps8 fragments. To verify that the binding was direct, purified His-tagged IRSp53-WT was used (the purity is shown in the left-end lane in Fig. 2C). Significant signals of bound IRSp53 were identified by Coomassie Blue staining in the lanes with GST-Eps8-1, -1-3, and -Pr (Fig. 2C), all of which contained the proline-rich sequence. These results indicate clearly that Eps8 binds directly to the IRSp53 SH3 domain via its proline-rich sequence in the NH<sub>2</sub>-terminal region.

**Cooperative Activation of Rac by the IRSp53/Eps8 Complex.**

As described above, Eps8 has been implicated in the regulation of Rac. This observation prompted us to investigate the possible involvement of IRSp53 in the regulation of Rac. To analyze the amount of activated Rac, a pull-down assay with GST-PAK-CRIB was used, because the CRIB motif of PAK selectively binds activated Rac (27, 28). From lysates of COS7 cells expressing Myc-Rac-WT (as an indicator) with FLAG-IRSp53-WT or FLAG-Eps8-WT, we did not identify any significant change in the amount of precipitated Myc-Rac-WT (Fig. 3A), consistent with previous reports of Eps8 (23). Surprisingly, when both Myc-IRSp53-WT and FLAG-Eps8-WT were coexpressed with Myc-Rac-WT, the level of activated Rac increased dramatically (Fig. 3B). This phenomenon was observed also when we coexpressed Myc-IRSp53-CT, but not Myc-IRSp53-ΔCT, instead of Myc-IRSp53-WT. These results suggest a positive interaction between IRSp53 and Eps8 in the regulation of Rac.

We hypothesized that an Eps8/Abi-1/Sos-1 Rac-guanine nucleotide exchange factor complex formation is stimulated by IRSp53/Eps8 interaction. To verify this hypothesis, pull-down assays were performed with GST-Abi-1-WT from lysates of COS7 cells expressing FLAG-Eps8-WT alone or with Myc-IRSp53-WT. We found that the amount of precipitated FLAG-Eps8 and Sos-1 increased significantly when Myc-IRSp53-WT was coexpressed, which was also precipitated (Fig. 3C). Taken together, we concluded that the interaction of IRSp53 with Eps8 augments Eps8/Abi-1/Sos-1 trimolecular complex formation, resulting in activation of Rac.

**Essential Role of the IRSp53/Eps8 Complex in Rac-Induced Rac Activation.**

On the basis of the findings described above and our initial characterization of IRSp53 as the downstream effector of Rac, Rac-induced Rac activation through IRSp53 and Eps8 was hypothesized. Then, we investigated whether the dominant-active form of Rac, Rac1G12V (Rac-DA), is able to induce Rac activation. Lysates from COS7 cells expressing Myc-Rac-WT (as an indicator) and FLAG-Rac-DA were prepared and subjected to pull-down assays with GST-PAK-CRIB. Indeed, there was a significant increase in the amount of activated Myc-Rac-WT compared with that of cell lysates expressing Myc-Rac-WT alone (Fig. 4A), indicating that dominant active form of Rac can induce Rac activation. Next, we investigated whether the IRSp53/Eps8 complex is involved in this Rac-induced Rac activation. We used the Eps8-1 fragment, which binds to the SH3 domain of IRSp53 and should inhibit complex formation between IRSp53 and Eps8. We coexpressed FLAG-Rac-DA and Myc-Rac-WT with or without FLAG-Eps8-1 in COS7 cells and investigated the effect on Rac activation. The levels of activated Myc-Rac-WT were decreased significantly when FLAG-Eps8-1 was coexpressed (Fig. 4B). Coexpression of FLAG-Eps8-WT or FLAG-Eps8-1-ΔPr did not decrease the levels of activated Rac, suggesting that IRSp53/Eps8 complex is important for Rac-induced

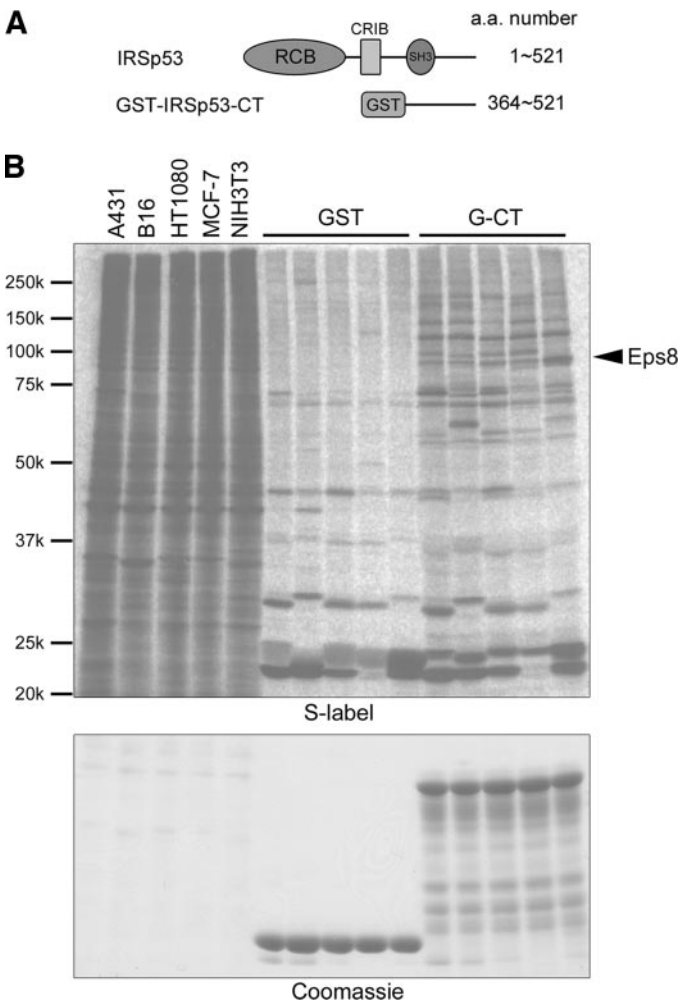


Fig. 1. Identification of Eps8 as an IRSp53-SH3 domain-binding protein in various cell lines. A, schematic of IRSp53 and glutathione S-transferase (GST)-IRSp53-CT structures. B, [<sup>35</sup>S]-labeled cell lysates were mixed with GST or GST-IRSp53-CT immobilized on beads, and bound proteins were subjected to SDS-PAGE. Gels were dried and analyzed by autoradiography. Arrowhead indicates Eps8. RCB, Rac-binding.

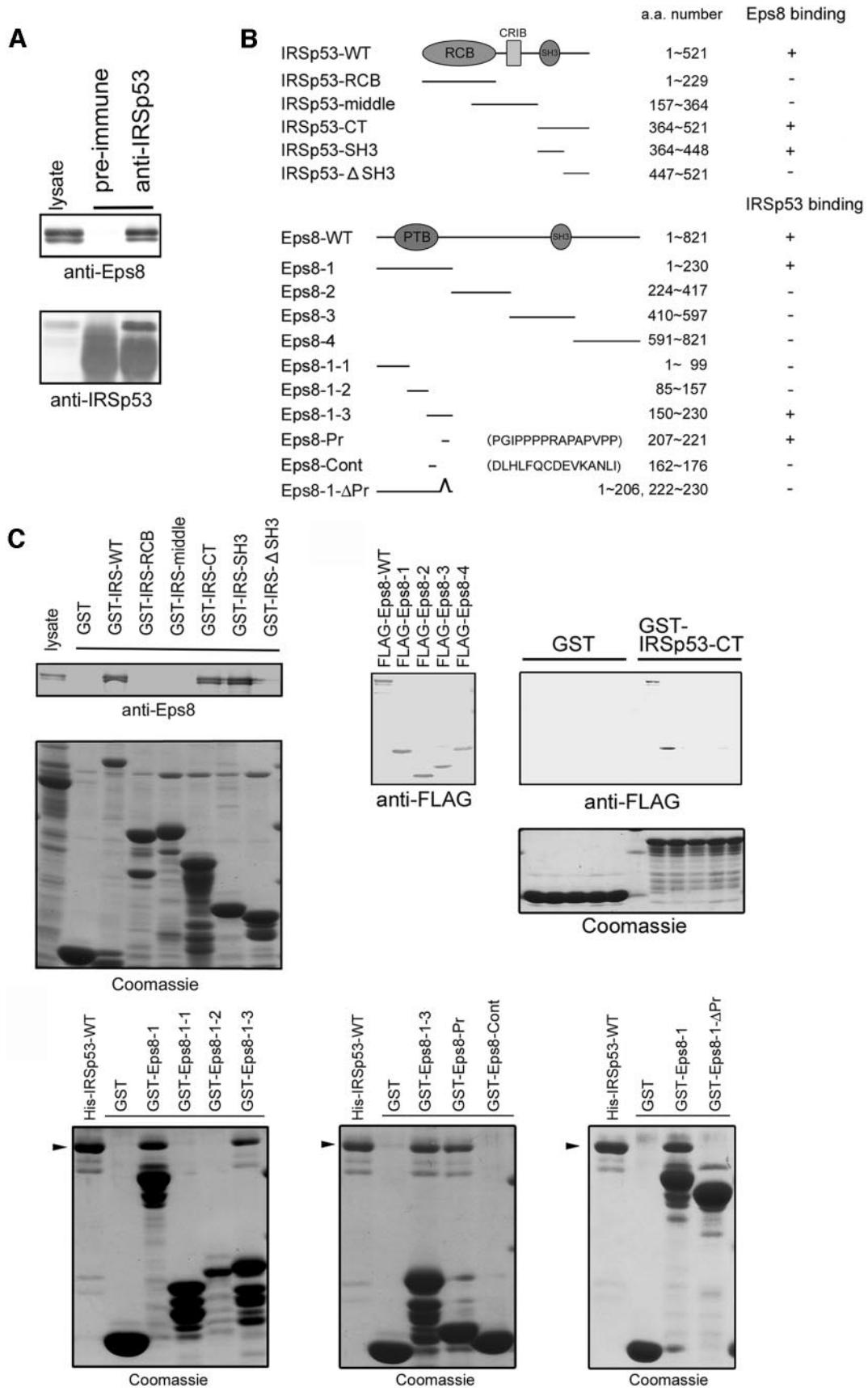


Fig. 2. *In vivo* and *in vitro* association between IRSp53 and Eps8. A, NIH3T3 cell lysates were subjected to immunoprecipitation analysis with anti-IRSp53 antibody (or control preimmune rabbit serum). Immunoprecipitated proteins were analyzed by Western blotting with anti-IRSp53 or anti-Eps8 antibodies. B, schematic of WT structure, various deletion mutants of IRSp53, and Eps8. Amino acid numbers are shown. The binding ability of Eps8 or IRSp53 is indicated also as “+” (positive) or “-” (negative). C, protein samples were subjected to pull-down assays with various GST-fusion proteins. Proteins bound to beads were analyzed by Western blotting or by Coomassie Blue staining. His-IRSp53-WT is indicated by arrowhead.

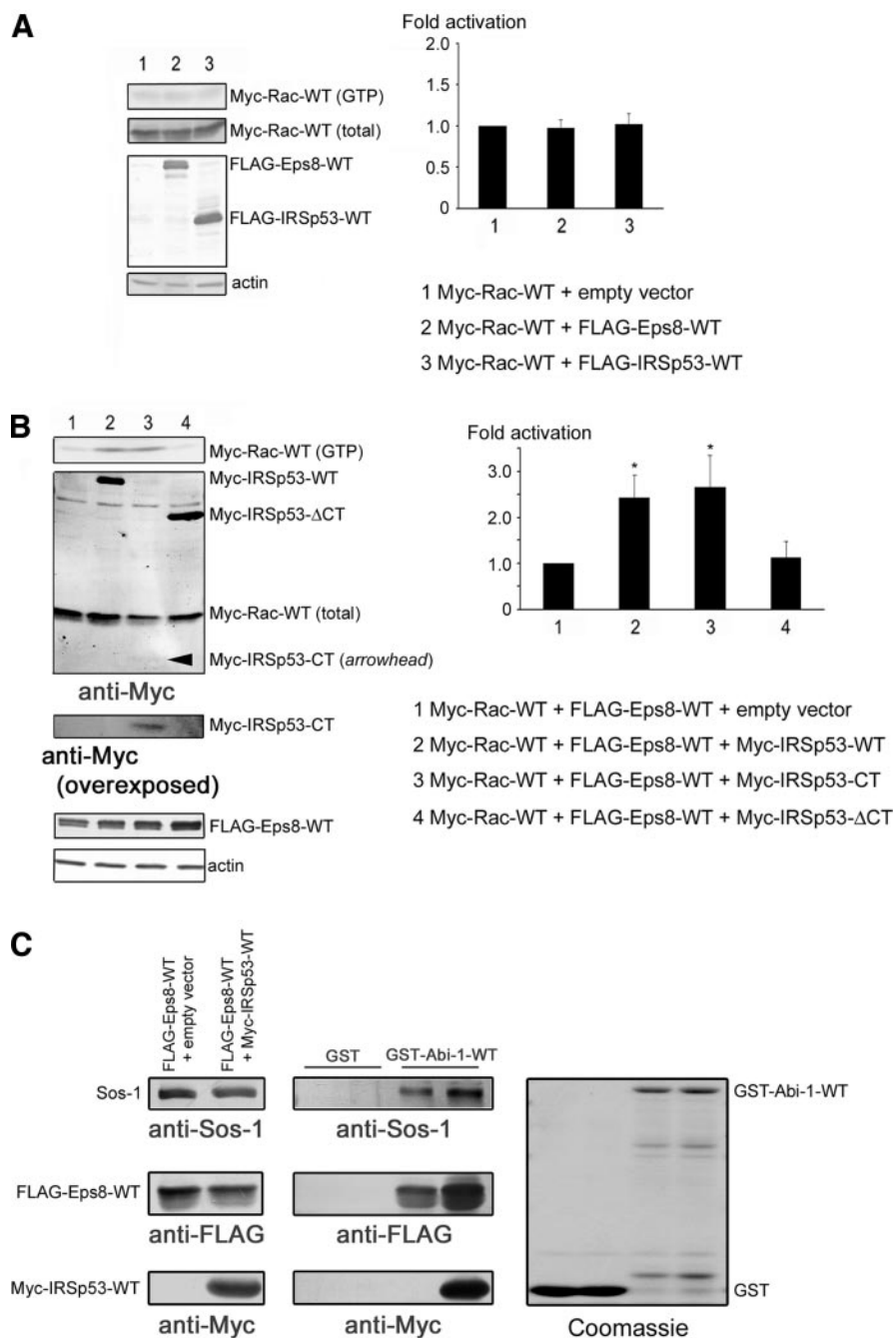


Fig. 3. Cooperative activation of Rac by IRSp53 and Eps8. **A**, Myc-Rac-WT, alone or with FLAG-Eps8-WT or FLAG-IRSp53-WT, was expressed in COS7 cells. Lysates were mixed with glutathione *S*-transferase (GST)-PAK-CRIB immobilized on beads. Bound Myc-Rac-WT was detected by anti-Myc antibody. Data are shown as mean  $\pm$  SE. **B**, lysates of COS7 cells expressing Myc-Rac-WT and FLAG-Eps8-WT, with or without Myc-IRSp53 (WT, CT, or  $\Delta$ CT), were subjected to pull-down assays with GST-PAK-CRIB as described in **A**. Activity of Rac are shown as mean  $\pm$  SE. \*,  $P < 0.05$  compared with the activation rate of cells expressing Myc-Rac-WT and FLAG-Eps8-WT. **C**, lysates of COS7 cells expressing FLAG-Eps8-WT, alone or with Myc-IRSp53-WT, were subjected to pull-down assay with GST-Abi-1-WT. Bound FLAG-Eps8-WT, Myc-IRSp53-WT, and Sos-1 were detected by anti-FLAG, anti-Myc, or anti-Sos-1 antibodies, respectively.

Rac activation. To confirm the inhibition of the IRSp53/Eps8 complex formation by FLAG-Eps8-1, immunoprecipitation analysis was performed also with lysates of COS7 cell expressing Myc-IRSp53, FLAG-Eps8-WT, and with or without FLAG-Eps8-1. We observed that the positive signal of FLAG-Eps8-WT in the anti-Myc immunoprecipitates clearly disappeared by the coexpression of FLAG-Eps8-1 (Fig. 4C), and FLAG-Eps8-1 was instead coimmunoprecipitated, which suggests that FLAG-Eps8-WT was competed away by FLAG-Eps8-1. Taken together, these results implicate the IRSp53/Eps8 complex in Rac-induced Rac activation.

**IRSp53/Eps8 Complex at the Leading Edge of Motile NIH3T3 Cells.** Next, we wanted to investigate the localization of the IRSp53/Eps8 complex inside motile cells. We used FRET analysis, because this method makes visible complex formation rather than colocalization. We used CFP-IRSp53 and YFP-Eps8 as donor and acceptor,

respectively. The acceptor photobleaching method was selected to avoid the problem of bleed-through between excitation and emission channels (schematic of acceptor photobleaching is shown in Fig. 5A). We expressed CFP-IRSp53 and YFP-Eps8 in NIH3T3 cells, and a wound was made to generate motile cells. Moving cells were then fixed and observed. When we calculated  $FRET_{eff}$ , a significant  $FRET_{eff}$  signal was observed at the leading edge of the cells (ROI1;  $16.7 \pm 1.4\%$ ) compared with other areas inside the cells (ROI2;  $2.2 \pm 1.3\%$ ; FRET efficiency included ROI1 and the aggregation of expressed proteins observed elsewhere in the cells; Fig. 5B). There was no significant  $FRET_{eff}$  signal in cells expressing CFP-IRSp53 with YFP or YFP-Eps8- $\Delta$ Pr and also in cells expressing YFP-Eps8 with CFP or CFP-IRSp53- $\Delta$ CT (Fig. 5B). These observations indicate clearly that IRSp53/Eps8 complex formation and, most likely, Rac-induced Rac activation occur at the leading edge of motile cells.

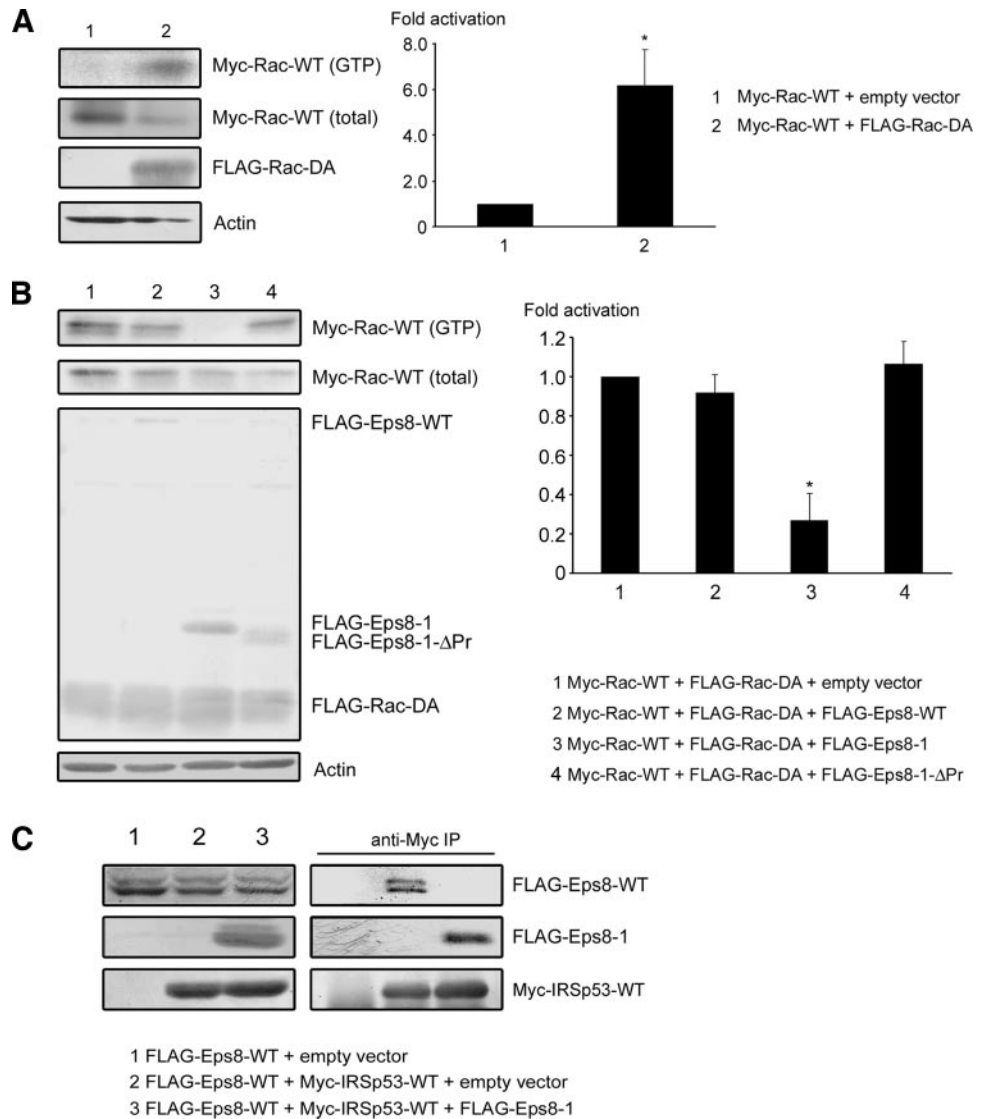


Fig. 4. Rac-induced Rac activation through IRSp53/Eps8 complex. *A*, Myc-Rac-WT, alone or with FLAG-Rac-DA, was expressed in COS7 cells. Lysates were subjected to pull-down assay with GST-PAK-CRIB, and the levels of activated Myc-Rac-WT were detected by anti-Myc antibody. Activity of Rac are shown as mean  $\pm$  SE. \*,  $P < 0.05$  compared with the activation rate of cells expressing Myc-Rac-WT alone. *B*, the levels of activated Myc-Rac-WT were investigated in lysates of COS7 cells expressing FLAG-Eps8-1, FLAG-Eps8-WT, FLAG-Eps8-1-ΔPr, or empty vector with Myc-Rac-WT and FLAG-Rac-DA. Arrowhead indicates FLAG-Rac-DA. Activity of Rac are shown as mean  $\pm$  SE. \*,  $P < 0.05$  compared with the activation rate of cells expressing Myc-Rac-WT and FLAG-Rac-DA. *C*, cell lysates of COS7 cells expressing Myc-IRSp53, FLAG-Eps8-WT, and with or without FLAG-Eps8-1 were subjected to immunoprecipitation using anti-Myc antibody. The amounts of Myc-IRSp53, FLAG-Eps8-WT, and FLAG-Eps8-1 in the immunoprecipitates were analyzed by Western blotting.

**Suppressed Motility and Invasiveness of HT1080 Cells by Inhibition of the IRSp53/Eps8 Complex.** The FRET observations suggested that the IRSp53/Eps8 complex is involved in cell motility, presumably through the positive regulation of Rac-activity. Therefore, we planned to analyze the possible role of the IRSp53/Eps8 complex in cell motility. First, we looked at the amount of activated Rac in various cell lines, which we found in the early experiments that Eps8 is probably present (Fig. 1*B*). By pull-down assays using GST-PAK-CRIB, we found that Rac inside HT1080 cells is activated strongly compared with other cell lines (Fig. 6*A*). This high Rac activity in HT1080 cells is consistent with the findings that HT1080 cells possess an oncogenic mutation in the *N-ras* gene and show high motility and invasion (29–31). Thus, we decided to use these HT1080 cells to analyze the importance of the IRSp53/Eps8 complex in cell motility.

HT1080 cells were transfected, then seeded onto colloidal gold-coated coverslips, and allowed to migrate for 12 h. Fixed cells were visualized by anti-FLAG antibody, and the area of the tracks of expressing cells was calculated. Cell motility was suppressed significantly by FLAG-Eps8-1 expression but not by FLAG-Eps8-WT or FLAG-Eps8-1-ΔPr expression (Fig. 6, *B* and *C*). In order to eliminate the possibility that the suppression was attributable to blockade of the interaction between IRSp53 and some other SH3 domain binding partners, such as WAVE2, the effect of FLAG-Eps8-ΔPr lacking the

NH<sub>2</sub>-terminal proline-rich sequence that binds IRSp53 was also investigated (schematic of Eps8-ΔPr structure is shown in Fig. 6*B*). FLAG-Eps8-ΔPr inhibited motility to a similar level as FLAG-Eps8-1 or FLAG-Rac-DN, suggesting that the IRSp53/Eps8 complex is important for cell motility.

We also performed Boyden chamber assays to determine cell motility and invasiveness. The transfection efficiency of HT1080 cells was checked by green fluorescent protein (GFP) fluorescence; it was 70–80% (data not shown). For counting the number of migrated cells, however, we used crystal violet staining instead of GFP fluorescence, because the GFP fluorescence from cells on the lower side of the chamber was too faint to allow for adequate quantification of the cells. Expression of GFP-Eps8-1 or GFP-Eps8-ΔPr (but not GFP-Eps8-WT or GFP-Eps8-1-ΔPr) suppressed cell migration and invasiveness toward the lower side of the chamber. The difference in the migration assay was weak, but the decreased level was statistically significant and was comparable with that of cells expressing GFP-Rac-DN (Fig. 6*D*), which is consistent with the phagokinetic track assay results. Interestingly, the decrease of invading cell number in the invasion assay was significantly greater than that in the migration assay (Fig. 6*D*). There was no significant difference in the proliferation rate of expressing cells by bromodeoxyuridine incorporation assay (data not shown), suggesting that the decreased number of invading cells ex-

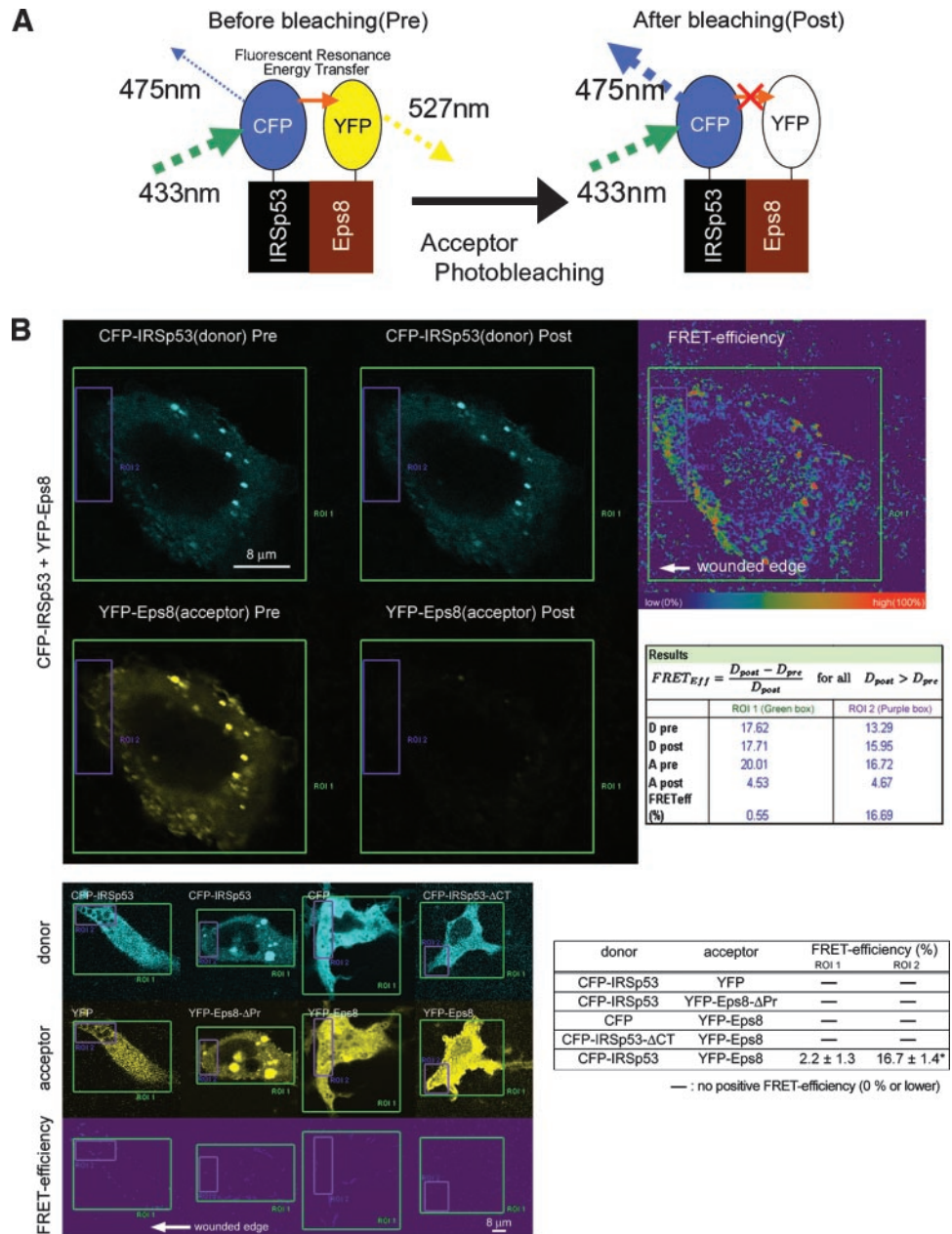


Fig. 5. IRSp53/Eps8 complex at the leading edge of motile NIH3T3 cells. **A**, schematic representation of FRET determination by acceptor photobleaching method. First, the emission intensity from CFP-IRSp53 ( $D_{pre}$ ) was acquired. Then, YFP-Eps8 was photobleached by repeated scanning with 514-nm light. After photobleaching, the emission intensity from CFP-IRSp53 ( $D_{post}$ ) was again acquired. If FRET has occurred, the emission intensity from CFP-IRSp53 after photobleaching ( $D_{post}$ ) should become stronger than that before ( $D_{pre}$ ), because the emission signal that has been consumed by YFP-Eps8 for FRET is also emitted. **B**, confluent NIH3T3 cells were transfected with CFP-IRSp53 and YFP-Eps8. At 24 h after transfection, a wound was made by a pipette tip, and 8 h later they were fixed. FRET signals of motile NIH3T3 cells were observed by acceptor photobleaching method. ROI1 is the area photobleached. The FRET efficiency ( $FRET_{eff}$ ) of ROI1 and ROI2 was calculated as  $FRET_{eff} = [D_{post} - D_{pre}] / D_{post}$  (the area without positive donor signal was excluded for calculation). The arrow indicates the moving direction of the cell. Similar results were obtained from three individual experiments, and in each experiment, all of the observed cells showed the similar tendency. The statistic data of  $FRET_{eff}$  in ROI2 (leading edge area; 10% from the tip of the cells) and ROI1 (inside the whole cell) are shown in the table below the figure as mean  $\pm$  SE. \*,  $P < 0.05$  compared with ROI1.

pressing GFP-Eps8-1 or GFP-Eps8-ΔPr detected in this assay was not because of the proliferation rate. These results support the notion that the IRSp53/Eps8 complex is especially important for the invasive behavior of HT1080 cells.

**DISCUSSION**

In this study, we identified Eps8 as the major binding protein for IRSp53 in NIH3T3 fibroblast cells and various cancer cell lines. Complex formation of endogenous IRSp53 and Eps8 was also confirmed. Taken together with the results of the functional characterization of the IRSp53/Eps8 complex, we propose that Eps8 is a novel functional partner for IRSp53. We reported previously that IRSp53 is an adaptor protein that functions downstream of Rac (9, 10), and the results presented above indicate an additional role for IRSp53 as an upstream regulator of Rac. Thus, we concluded that IRSp53 is a bifunctional molecule and may mediate positive feedback on the Rac signal.

A positive regulation of Rac via IRSp53/Eps8 complex may

underlie the spontaneous formation of polarity by neutrophils in response to chemoattractants, which has been observed in previous studies (32, 33). Although the authors have shown that the activation of the phosphatidylinositol 3'-OH kinase (PI3k) is important for it, the precise mechanism has not been revealed completely. Several possibilities can be considered about the relevance between PI3k-mediated Rac-activation and IRSp53/Eps8 complex-mediated Rac-activation. There is a report suggesting that inhibition of PI3k activity cannot suppress polarity formation completely (34). Therefore, the IRSp53/Eps8 complex-mediated Rac-activation can be a novel route for positive feedback regulation of Rac, which can compensate the PI3k-mediated Rac-activation. Another case is that the IRSp53/Eps8 complex plays a regulatory role during the PI3k-mediated Rac-activation. Indeed, Abi-1, an essential component of the Eps8-containing guanine nucleotide exchange factor for Rac, has been reported to associate with the p85 subunit of PI3k (25). Therefore, it may be possible that IRSp53 also participates in the complex formation with PI3k through

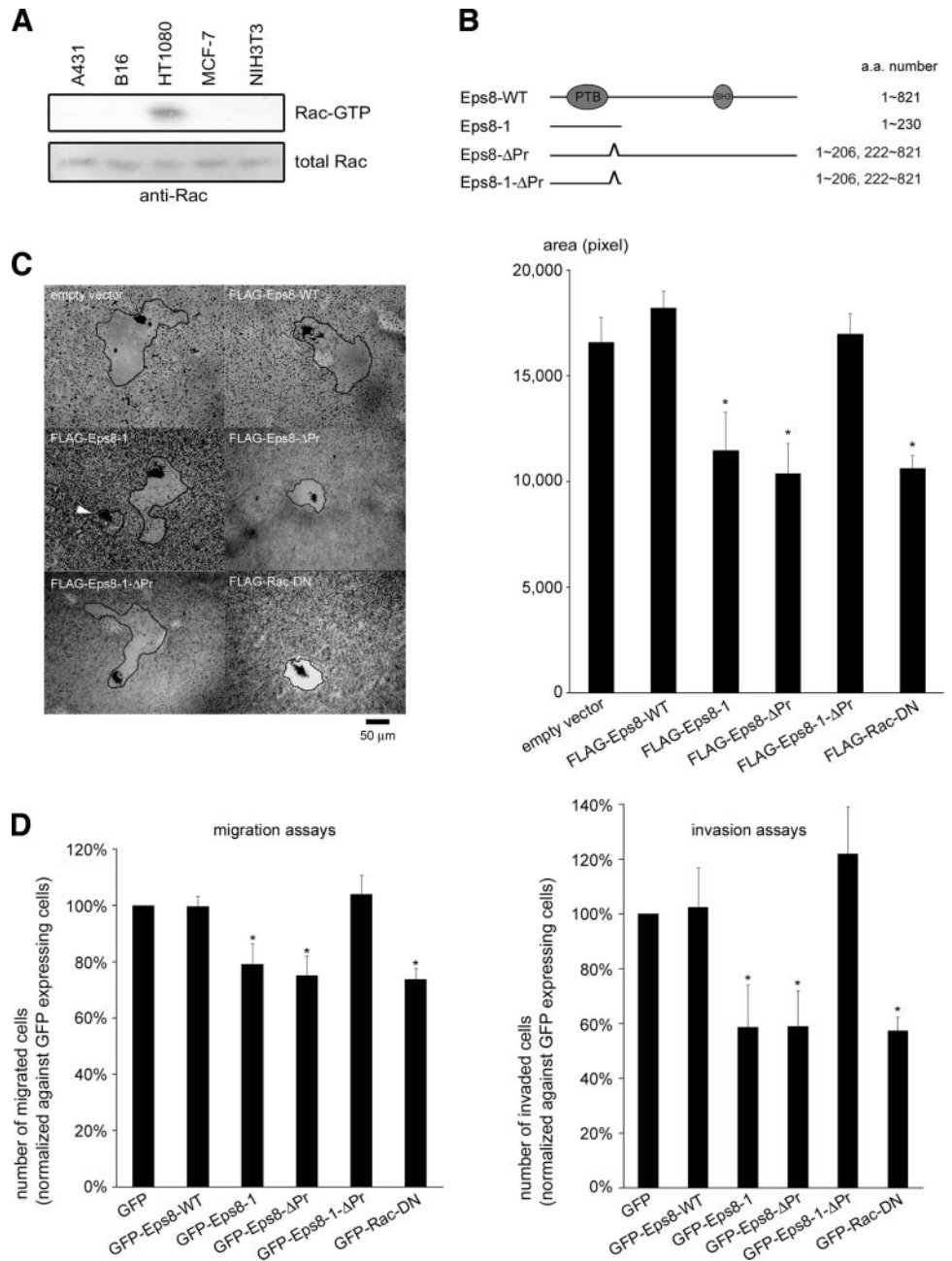


Fig. 6. Suppressed motility and invasiveness of HT1080 cells expressing Eps8-1 or Eps8-ΔPr. **A**, lysates were subjected to pull-down assays using GST-PAK-CRIB. Precipitated endogenous Rac were detected by anti-Rac antibody. **B**, schematic of Eps8-1, Eps8-ΔPr, and Eps8-1-ΔPr structures. **C**, HT1080 cells were transfected with FLAG-Eps8-WT, FLAG-Eps8-1, FLAG-Eps8-ΔPr, FLAG-Eps8-1-ΔPr, or FLAG-Rac-DN (FLAG-Rac1T17N), and then cultured for 12 h on colloidal gold-coated coverslips. Cells were stained with anti-FLAG antibody to visualize cells expressing FLAG-tagged constructs (in FLAG-Eps8-1 panel, only the cell pointed with an arrowhead is expressing). Each area of the tracks (indicated as areas surrounded by lines) was calculated by NIH image. The areas of the tracks by three independent assays are shown as mean ± SE. \*,  $P < 0.05$  compared with the migrated area of empty vector, FLAG-Eps8-WT, or FLAG-Eps8-1-ΔPr-expressing cells. **D**, transfected HT1080 cells were seeded on the upper membrane of Boyden chambers. Fixed cells on the lower side were then stained with crystal violet. The number of the cells were counted and normalized against the number of green fluorescent protein (GFP)-expressing cells. Data are shown as mean ± SE. \*,  $P < 0.05$  compared with the number of migrated GFP, GFP-Eps8-WT, or GFP-Eps8-1-ΔPr-expressing cells.

Eps8 and Abi-1 and exerts some regulatory effect on it. Now, we do not possess a clear answer to this problem, which should be the focus for future studies.

One important question is whether the IRSp53/Eps8 complex formation is regulated by external cues, such as growth factors. We performed coimmunoprecipitation analysis with lysates from growth factor-stimulated or mock-stimulated cells, although we have not found a significant difference in the amount of the complex (data not shown). However, we do not think that this result does not necessarily exclude the possibility that the complex formation is regulated dynamically *in vivo*, because lysis procedure destroys the cytoskeletal structure such as those seen at the leading edge, which may be required for maintaining the complex. More careful examination may be needed to solve this problem. In addition, it is possible that the signal transduction via the IRSp53/Eps8 complex is regulated by extracellular stimuli. The simplest scenario is that the localization of the complex may be regulated. Accumulation of the IRSp53/Eps8

complex above some threshold level may be necessary for maintaining Rac activation at the leading edge and after cell movement. Additionally, both IRSp53 and Eps8 were identified originally as substrates for tyrosine kinases activated by extracellular stimulation (35, 17). Thus, it is possible that Rac-activating ability of the IRSp53/Eps8 complex is regulated by tyrosine phosphorylation. Many additional studies will be required to clarify the mechanism of IRSp53/Eps8 complex mediated signaling.

**ACKNOWLEDGMENTS**

We thank Dr. Shiro Suetsugu (University of Tokyo, Tokyo, Japan) for the Abi-1 cDNA construct and Dr. Toshifumi Azuma for the anti-Rac antibody.

**REFERENCES**

1. Ridley AJ, Paterson HF, Johnston CL, Diekmann D, Hall A. The small GTP-binding protein rac regulates growth factor-induced membrane ruffling. *Cell* 1992;70:401-10.

2. Etienne-Manneville S, Hall A. Rho GTPases in cell biology. *Nature (Lond)* 2002; 420:629–35.
3. Sahai E, Marshall CJ. RHO-GTPases and cancer. *Nat Rev Cancer* 2002;2:133–42.
4. Miki H, Suetsugu S, Takenawa T. WAVE, a novel WASP-family protein involved in actin reorganization induced by Rac. *EMBO J* 1998;17:6932–41.
5. Suetsugu S, Miki H, Takenawa T. Identification of two human WAVE/SCAR homologues as general actin regulatory molecules which associate with the Arp2/3 complex. *Biochem Biophys Res Commun* 1999;260:296–302.
6. Yan C, Martinez-Quiles N, Eden S, et al. WAVE2 deficiency reveals distinct roles in embryogenesis and Rac-mediated actin-based motility. *EMBO J* 2003;22:3602–12.
7. Yamazaki D, Suetsugu S, Miki H, et al. WAVE2 is required for directed cell migration and cardiovascular development. *Nature (Lond)* 2003;424:452–6.
8. Suetsugu S, Yamazaki D, Kurisu S, Takenawa T. Differential roles of WAVE1 and WAVE2 in dorsal and peripheral ruffle formation for fibroblast cell migration. *Dev Cell* 2003;5:595–609.
9. Miki H, Yamaguchi H, Suetsugu S, Takenawa T. IRSp53 is an essential intermediate between Rac and WAVE in the regulation of membrane ruffling. *Nature (Lond)* 2000;408:732–5.
10. Miki H, Takenawa T. WAVE2 serves a functional partner of IRSp53 by regulating its interaction with Rac. *Biochem Biophys Res Commun* 2002;293:93–9.
11. Nakagawa H, Miki H, Nozumi M, et al. IRSp53 is colocalised with WAVE2 at the tips of protruding lamellipodia and filopodia independently of Mena. *J Cell Sci* 2003;116:2577–83.
12. Govind S, Kozma R, Monfries C, Lim L, Ahmed S. Cdc42Hs facilitates cytoskeletal reorganization and neurite outgrowth by localizing the 58-kD insulin receptor substrate to filamentous actin. *J Cell Biol* 2001;152:579–94.
13. Krugmann S, Jordens I, Gevaert K, et al. Cdc42 induces filopodia by promoting the formation of an IRSp53:Mena complex. *Curr Biol* 2001;11:1645–55.
14. Bockmann J, Kreutz MR, Gundelfinger ED, Bockers TM. ProSAP/Shank postsynaptic density proteins interact with insulin receptor tyrosine kinase substrate IRSp53. *J Neurochem* 2002;83:1013–7.
15. Soltau M, Richter D, Kreienkamp HJ. The insulin receptor substrate IRSp53 links postsynaptic shank1 to the small G-protein cdc42. *Mol Cell Neurosci* 2002;21:575–83.
16. Fujiwara T, Mammoto A, Kim Y, Takai Y. Rho small G-protein-dependent binding of mDia to an Src homology 3 domain-containing IRSp53/BAIAP2. *Biochem Biophys Res Commun* 2000;271:626–9.
17. Fazioli F, Minichiello L, Matoska V, et al. Eps8, a substrate for the epidermal growth factor receptor kinase, enhances EGF-dependent mitogenic signals. *EMBO J* 1993; 12:3799–808.
18. Matoskova B, Wong WT, Salcini AE, Pelicci PG, Di Fiore PP. Constitutive phosphorylation of eps8 in tumor cell lines: relevance to malignant transformation. *Mol Cell Biol* 1995;15:3805–12.
19. Maa MC, Hsieh CY, Leu TH. Overexpression of p97Eps8 leads to cellular transformation: implication of pleckstrin homology domain in p97Eps8-mediated ERK activation. *Oncogene* 2001;20:106–12.
20. Gallo R, Provenzano C, Carbone R, et al. Regulation of the tyrosine kinase substrate Eps8 expression by growth factors, v-Src and terminal differentiation. *Oncogene* 1997;15:1929–36.
21. Maa MC, Lai JR, Lin RW, Leu TH. Enhancement of tyrosyl phosphorylation and protein expression of eps8 by v-Src. *Biochim Biophys Acta* 1999;1450:341–51.
22. Biesova Z, Piccoli C, Wong WT. Isolation and characterization of e3B1, an eps8 binding protein that regulates cell growth. *Oncogene* 1997;14:233–41.
23. Scita G, Tenca P, Areces LB, et al. An effector region in Eps8 is responsible for the activation of the Rac-specific GEF activity of Sos-1 and for the proper localization of the Rac-based actin-polymerizing machine. *J Cell Biol* 2001;154:1031–44.
24. Scita G, Nordstrom J, Carbone R, et al. EPS8 and E3B1 transduce signals from Ras to Rac. *Nature (Lond)* 1999;401:290–3.
25. Innocenti M, Frittoli E, Ponzanelli I, et al. Phosphoinositide 3-kinase activates Rac by entering in a complex with Eps8, Abi1, and Sos-1. *J Cell Biol* 2003;160:17–23.
26. Mori H, Tomari T, Koshikawa N, et al. CD44 directs membrane-type 1 matrix metalloproteinase to lamellipodia by associating with its hemopexin-like domain. *EMBO J* 2002;21:3949–59.
27. Manser E, Leung T, Salihuddin H, Zhao ZS, Lim L. A brain serine/threonine protein kinase activated by Cdc42 and Rac1. *Nature (Lond)* 1994;367:40–6.
28. Akasaki T, Koga H, Sumimoto H. Phosphoinositide 3-kinase-dependent and -independent activation of the small GTPase Rac2 in human neutrophils. *J Biol Chem* 1999;274:18055–9.
29. Rasheed S, Nelson-Rees WA, Toth EM, Arnstein P, Gardner MB. Characterization of a newly derived human sarcoma cell line (HT-1080). *Cancer (Phila)* 1974;33: 1027–33.
30. Hall A, Marshall CJ, Spurr NK, Weiss RA. Identification of transforming gene in two human sarcoma cell lines as a new member of the ras gene family located on chromosome 1. *Nature (Lond)* 1983;303:396–400.
31. Brown R, Marshall CJ, Pennie SG, Hall A. Mechanism of activation of an N-ras gene in the human fibrosarcoma cell line HT1080. *EMBO J* 1984;3:1321–6.
32. Weiner OD, Neilsen PO, Prestwich GD, et al. A PtdInsP(3)- and Rho GTPase-mediated positive feedback loop regulates neutrophil polarity. *Nat Cell Biol* 2002;4: 509–13.
33. Wang F, Herzmark P, Weiner OD, et al. Lipid products of PI(3)Ks maintain persistent cell polarity and directed motility in neutrophils. *Nat Cell Biol* 2002;4:513–8.
34. Funamoto S, Meili R, Lee S, Parry L, Firtel RA. Spatial and temporal regulation of 3-phosphoinositides by PI 3-kinase and PTEN mediates chemotaxis. *Cell* 2002;109: 611–23.
35. Yeh TC, Ogawa W, Danielsen AG, Roth RA. Characterization and cloning of a 58/53-kDa substrate of the insulin receptor tyrosine kinase. *J Biol Chem* 1996;271: 2921–8.